World Journal of Pharmaceutical Science and Research

www.wjpsronline.com

Research Article

ISSN: 2583-6579
SJIF Impact Factor: 6.916
Year - 2026
Volume: 5; Issue: 8
Page: 870-889

A STABILITY-INDICATING RP-HPLC METHOD DEVELOPMENT AND VALIDATED ACROSS FOUR BIORELEVANT MATRICES FOR AZELNIDIPINE–TELMISARTAN

Battula Sammaiah*, Dr. K. Ram Prasad

Research Scholar, Faculty of Pharmaceutical Sciences, Motherhood University, Dehradun Road, Karoundi Village, Bhagwanpur Post, Roorkee Tehsil, Haridwar District, Uttarakhand 247661.

Article Received: 06 July 2026 | | Article Revised: 27 July 2026 | | Article Accepted: 16 August 2026

***Corresponding Author: Battula Sammaiah**
Research Scholar, Faculty of Pharmaceutical Sciences, Motherhood University, Dehradun Road, Karoundi Village, Bhagwanpur Post, Roorkee Tehsil, Haridwar District, Uttarakhand 247661. **DOI:** https://doi.org/10.5281/zenodo.21978937

How to cite this Article: Battula Sammaiah, Dr. K. Ram Prasad (2026) A STABILITY-INDICATING RP-HPLC METHOD DEVELOPMENT AND VALIDATED ACROSS FOUR BIORELEVANT MATRICES FOR AZELNIDIPINE–TELMISARTAN. World Journal of Pharmaceutical Science and Research, 5(8), 870-889.

ABSTRACT

Azelnidipine (AZL) and telmisartan (TEL) are both BCS Class II antihypertensives of high lipophilicity (logP 4.5 and 7.7), co-formulated as a once-daily fixed-dose combination (FDC) whose oral performance is governed by solubility rather than permeability. Existing chromatographic methods for the pair quantify tablet content in simple buffers; none has asked how the bile-salt micellar environment of the intestinal lumen reshapes either the degradation chemistry or the dissolution behaviour of the two drugs. We developed a single isocratic reversed-phase HPLC method — Inertsil ODS-3 (250 × 4.6 mm, 5 µm), acetonitrile: 0.1% ortho-phosphoric acid (pH 3.0), 60:40 (v/v), 1.0 mL min^{-1}, 30 °C, 240 nm, 10 min — and validated it in four matrices (diluent, FaSSGF, FaSSIF-V2, FeSSIF-V2) per ICH Q2(R1)/Q2(R2). Working concentrations of 17.78 µg mL^{-1} (AZL) and 44.44 µg mL^{-1} (TEL) corresponded to complete label-dose release into the 900 mL compendial vessel. Resolution reached 7.92; every validation figure of merit passed in every matrix ($r^2 \geq 0.9999$; recovery 99.11–99.90%; pooled precision %RSD ≤ 0.89%). Forced degradation was run under six ICH stress conditions in diluent and, as the analytical departure of this work, repeated with each drug embedded in FaSSIF-V2 and FeSSIF-V2 micelles. The fed-state medium attenuated AZL degradation by 4.0–5.5 percentage points and TEL degradation by 4.3–7.8 percentage points, the protection scaling with taurocholate concentration — a magnitude far above what freely soluble drugs experience, and consistent with near-complete partitioning of both high-logP molecules into the micelle core. No matrix-specific degradant appeared; the micelle changed rate, not pathway. Biorelevant dissolution exposed a striking release contrast: at 15 min TEL reached 85.5% in FeSSIF-V2 against 23.8% in compendial 0.1 N HCl, an ≈ 62 percentage-point gap, with AZL showing the same fed-state acceleration. Both partners returned $f_2 < 50$ for fed-versus-fasted comparisons (AZL 34.98; TEL 27.46) — a bilateral in vitro food-effect signal not previously reported for this FDC. Tablet assay recovered 99.96% (AZL) and 99.88% (TEL) of label claim. The method couples full biorelevant-matrix validation with in-medium degradation probing for the first time in this drug pair, and the data argue for FeSSIF-V2 as a discriminating early-development screen for lipophilic antihypertensive combinations.

KEYWORDS: Azelnidipine; telmisartan; RP-HPLC; stability-indicating; biorelevant dissolution; FaSSIF-V2; FeSSIF-V2; bile-salt micelle; food effect; BCS Class II; fixed-dose combination; hypertension.

1. INTRODUCTION

Hypertension is the largest single modifiable driver of cardiovascular death worldwide. Reaching target pressure in most patients takes more than one agent, and the reason is mechanistic rather than incidental: the systems that raise arterial pressure are redundant, so blocking one axis provokes compensatory activation of the others, and monotherapy loses ground over time as those counter-regulatory loops reassert themselves. Combination therapy answers that redundancy head-on. Pairing a calcium-channel blocker with a renin–angiotensin blocker attacks two independent limbs of pressure control at once, and fixed-dose co-formulation folds the two into a single daily tablet — a formulation decision that matters clinically, because pill burden is one of the better-documented predictors of non-adherence in chronic antihypertensive care (Bangalore et al., 2007).

Azelnidipine and telmisartan make a considered pair. AZL is a third-generation dihydropyridine that blocks L-type calcium channels with a slow onset and long duration, producing sustained vasodilation without the reflex tachycardia that troubles earlier agents in the class; TEL is an angiotensin II AT_1-receptor blocker with the longest plasma half-life of the sartans and partial PPAR-γ agonism that may carry metabolic benefit (Kario et al., 2013; Sasaki et al., 2024). Their once-daily fixed-dose combination is marketed in India and Japan and has shown favourable ambulatory blood-pressure control against comparator regimens (Kario et al., 2013). What unites them pharmaceutically, though, is a shared liability. Both are BCS Class II — high permeability, low solubility — and both are strongly lipophilic, AZL at logP 4.5 and TEL at an extreme logP of 7.7, with aqueous solubility below 1 μg mL^{-1} across the physiological pH range (Park et al., 2013; Pravalika & Kumar, 2021; Wu & Benet, 2005).

That shared Physico-chemistry is the crux. For a Class II drug, the rate-limiting step of oral absorption is dissolution, and dissolution in the small intestine is not governed by aqueous solubility alone — it hinges on the solubilizing capacity of bile-salt and lecithin micelles, whose concentration swings several-fold between the fasted and fed states (Galia et al., 1998; Jantratid et al., 2008; Mithani et al., 1996). A compendial buffer at pH 6.8 captures none of this. It reports a number with little bearing on what the tablet does in a fed duodenum. Second-generation biorelevant media — FaSSIF-V2 and FeSSIF-V2 — were built precisely to reproduce that micellar environment, and for lipophilic actives they routinely surface release behaviour that simple buffers cannot (Klein, 2010; Markopoulos et al., 2015). A second, less examined consequence of micellar partitioning deserves attention: a molecule sequestered inside a micelle is not only more soluble, it is also physically shielded from the bulk aqueous phase where hydrolytic and oxidative attack occurs. Whether that shielding measurably slows the degradation of AZL and TEL under stress is an open question — and one with direct bearing on how mass-balance and impurity data from biorelevant dissolution ought to be read.

Seven prior RP-HPLC reports address the AZL–TEL pair or AZL alone (Andrews et al., 2023; Bhandari & Bhangale, 2024; Nandyala et al., 2024; Parikh & Patel, 2025; Pravalika & Kumar, 2021; Sridhar et al., 2023; WJPS editorial team, 2022). Each validated tablet assay and a partial stress panel in conventional diluent or simple phosphate buffer. None repeated the stress challenges inside FaSSIF-V2 or FeSSIF-V2, and none generated a six-medium biorelevant dissolution data set spanning fasted-gastric, fasted-intestinal, fed-intestinal and the three compendial buffers for both partners at once. We set out to close that gap. The objectives were four: to develop an isocratic method resolving AZL and TEL cleanly in every dissolution matrix; to validate it across diluent, FaSSGF, FaSSIF-V2 and FeSSIF-V2 against the full ICH Q2(R1)/Q2(R2) set; to run forced degradation both in diluent and inside the two bile-salt media, testing

whether micellar occupancy protects the dihydropyridine and benzimidazole rings from chemical attack; and to profile biorelevant dissolution of the marketed FDC, comparing the resulting curves by the f_2 similarity metric.

2. MATERIALS AND METHODS

2.1 Reagents and Reference Standards

AZL and TEL working standards (≥ 99.5% purity, USP-traceable) were received as gift samples from a domestic API manufacturer. HPLC-grade acetonitrile, methanol, ortho-phosphoric acid (85% w/w), monobasic and dibasic phosphate salts, sodium chloride, sodium hydroxide, hydrochloric acid (35%), hydrogen peroxide (30% w/v) and pepsin (3,200 U mg^{-1}) came from Merck (Mumbai, India) and Sigma-Aldrich (St. Louis, MO, USA). Sodium taurocholate (≥ 97%), egg-yolk L-α-phosphatidylcholine (≥ 99%), glyceryl monooleate and sodium oleate — the constituents of FaSSGF, FaSSIF-V2 and FeSSIF-V2 — were from Sigma-Aldrich; ready-to-use SIF Powder Original and V2 (Biorelevant.com, London, UK) cross-verified the in-house media. Milli-Q water (18.2 MΩ·cm) was used throughout. AZL stocks were handled under amber glass and shielded from light, because the 1,4-dihydropyridine ring photo-oxidizes readily to its pyridine analogue (Pravalika & Kumar, 2021).

2.2 Instrumentation

Standard equipment throughout. Chromatographic analyses ran on a Shimadzu LC-2030C 3D Plus platform with a photodiode-array detector set to scan 190–400 nm, a 100-position thermostatted autosampler and a Peltier column oven (LabSolutions v5.97; Shimadzu, Kyoto, Japan); the PDA channel doubled as the peak-purity monitor during all method-development injections. Dissolution? Paddle only. An Electrolab TDT-08L USP Type II paddle apparatus (Electrolab, Mumbai, India) with stainless-steel spiral sinkers handled every dissolution run. Wavelength scans were recorded on a Shimadzu UV-1900 spectrophotometer; pH was measured on a Mettler Toledo S220 meter calibrated against NIST-traceable buffers (pH 4.01, 7.00, 10.00); weighing used a Mettler Toledo XSE205DU analytical balance (0.01 mg readability).

2.3 Chromatographic Conditions and Diluent

Separation was isocratic on an Inertsil ODS-3 C18 column (250 × 4.6 mm, 5 µm; GL Sciences) with acetonitrile: 0.1% v/v aqueous OPA (pH 3.0), 60:40 (v/v), at 1.0 mL min^{-1} and 30 °C; detection at 240 nm, 20 µL injection, 10 min run. Organic fraction matters here. A 60% acetonitrile content — well above what more polar drug pairs require — is dictated by TEL, whose logP of 7.7 demands strong eluotropic strength to elute inside 10 min on a C18 phase (Bhandari & Bhangale, 2024; Snyder et al., 2010). At pH 3.0 the TEL carboxylate (pKa 3.5) stays fully protonated and the weakly basic AZL (pKa ≈ 5.5) is fully ionized, so both elute as sharp, reproducible peaks with silanol interaction suppressed (Neue, 1997; Park et al., 2013). Filtration (0.45 µm nylon) and 15 min sonication completed mobile-phase preparation (USP, 2023a). Diluent was ACN: water (60:40, v/v), matched to eluent strength to prevent solvent-mismatch band distortion.

2.4 Biorelevant and Compendial Media

Three biorelevant media — FaSSGF (pH 1.6; 0.08 mM taurocholate, 0.02 mM lecithin, pepsin), FaSSIF-V2 (pH 6.5; 3 mM taurocholate, 0.2 mM lecithin) and FeSSIF-V2 (pH 5.8; 10 mM taurocholate, 2 mM lecithin, glyceryl monooleate, sodium oleate) — were constituted per Jantratid et al. (2008). Six media total. Three compendial buffers (0.1 N HCl pH 1.2, acetate pH 4.5, phosphate pH 6.8) completed the panel (USP, 2023c). All were equilibrated 1 h at 37.0 ± 0.5 °C and used within 24 h; pepsin entered FaSSGF only at the dissolution step, never in chromatographic samples.

2.5 Working Concentrations and Standard Preparation

Working concentrations followed directly from the compendial vessel geometry. A single FDC tablet (AZL 16 mg + TEL 40 mg) dissolving into the USP default 900 mL delivers 17.78 μg mL^{-1} AZL and 44.44 μg mL^{-1} TEL, holding the label-dose ratio at exactly 1: 2.5 (USP, 2023b, 2023c). Setting the assay concentration equal to the 100%-release concentration removes a dilution step from the dissolution workflow and cuts error propagation — the convention adopted by Andrews et al. (2023). Stocks (177.8 and 444.4 μg mL^{-1}) were stored at 4 °C in amber glass and used within seven days; combined working standards were freshly prepared daily.

2.6 Sample Preparation for Micellar Matrices

Micelles complicate everything downstream. Bile-salt/lecithin micelles partition lipophilic analytes and adsorb them to filter membranes simultaneously, and for BCS Class II actives the resulting under-recovery can be severe if the micellar phase is not disrupted before injection (Park et al., 2013; Pillay et al., 2018; Sugano & Takeru, 2023). Each aliquot (5 mL) was filtered through 0.45 μm PTFE with the first 2 mL discarded to saturate membrane binding sites; 1.0 mL filtrate was then mixed 1:1 with acetonitrile to precipitate lecithin and dissolve bile salts, releasing partitioned drug into the supernatant (Galia et al., 1998); FeSSIF-V2 samples required additional centrifugation (15,000 rpm, 10 min, 4 °C) to sediment residual lecithin solids before re-filtration and 20 μL injection. PTFE rather than PVDF — a deliberate departure from the polar-membrane default — was selected because the extreme lipophilicity of TEL drives strong, reproducibility-limiting adsorption onto PVDF surfaces (Park et al., 2013).

2.7 Wavelength Selection

UV scans (200–400 nm) placed AZL λmax at 254 nm and TEL λmax at 296 nm. A 42 nm separation between the two maxima means neither is usable for the partner: at 254 nm the TEL response falls by roughly a quarter, and at 296 nm the AZL signal all but vanishes. A compromise at 240 nm gave acceptable joint sensitivity while sitting safely above the ≈ 220 nm UV cut-off of bile salts and lecithin (Galia et al., 1998), and it aligns with the working wavelengths of Andrews et al. (2023) and Parikh and Patel (2025).

2.8 Systematic Chromatographic Optimization

Method development proceeded by sequential single-parameter evaluation — each variable studied in turn while the others were held at their best prior value (Snyder et al., 2010). Twenty-one trials spanned stationary phase (four C18 columns), organic modifier (acetonitrile versus methanol), aqueous pH (0.1% OPA at pH 3.0 and 2.5; phosphate at pH 4.5 and 6.8), organic proportion (ACN: OPA from 50:50 to 70:30), flow rate (0.8–1.2 mL min^{-1}) and column temperature (25–35 °C). Acceptance at each step required $R_s \geq 2.0$, tailing ≤ 2.0, $N \geq 2{,}000$, k' of 2–10 and run time ≤ 15 min (USP, 2023a).

2.9 Method Validation

Validation ran in four matrices per ICH Q2(R1) and Q2(R2) (ICH, 2005, 2023). Linearity used six levels (25–150% of working concentration) in triplicate; accuracy used spiked placebo at 50, 100 and 150% (nine determinations per matrix); repeatability used six replicates at 100%; intermediate precision used a two-day × two-analyst design (24 per matrix). LOD and LOQ came from the calibration-curve formulae ($3.3\sigma/S$ and $10\sigma/S$) cross-checked against signal-to-noise. The robustness study perturbed five parameters by one unit each (pH ± 0.2, ACN ± 2%, flow ± 0.1 mL min^{-1}, temperature ± 2 °C, wavelength ± 2 nm). Filter suitability compared PVDF, PTFE and Nylon against a centrifuge

reference; solution stability was checked at 25, 15 and 4 °C; matrix effect used the slope ratio against diluent (Matuszewski et al., 2003). Acceptance thresholds are consolidated in Table 1.

Table 1: Consolidated validation acceptance criteria and physicochemical profile of the two analytes.

Property / Parameter	Azelnidipine (AZL)	Telmisartan (TEL)
Therapeutic class	Dihydropyridine CCB (L-type)	Angiotensin II AT_1 blocker
Molecular weight (g mol⁻¹)	582.65	514.62
pKa	≈ 5.5 (basic, pyridyl N)	3.5 / 6.0 (carboxyl / imidazole)
logP	4.5	7.7
Aqueous solubility (25 °C)	< 1 µg mL⁻¹	< 0.1 µg mL⁻¹ (pH 3–7)
BCS class	II (low sol., high perm.)	II (low sol., high perm.)
Dose in FDC	16 mg	40 mg
Working concentration	17.78 µg mL⁻¹	44.44 µg mL⁻¹

2.10 Forced Degradation, Including In-Medium Stress

Six stress conditions. Stress testing followed ICH Q1A(R2)/Q1B and the Singh–Bakshi consensus, targeting 5–20% parent loss per condition (Bakshi & Singh, 2002; Blessy et al., 2014; ICH, 1996, 2003). Because both analytes are almost insoluble in water, acid and base stress samples carried 50% methanol as co-solvent — an approach explicitly endorsed for highly lipophilic actives by Bakshi and Singh (2002) and applied to this drug pair by Pravalika and Kumar (2021). Applied conditions in diluent were: acid (1 N HCl, 60 °C, 6 h), base (1 N NaOH, 60 °C, 6 h), oxidation (3% H_2O_2, RT, 24 h), thermal (80 °C, 72 h solid-state), photolysis (ICH Q1B Option 1) and humidity (25 °C/90% RH, 30 d). Acid, base and peroxide stresses were then repeated with each drug pre-dissolved in FaSSIF-V2 and FeSSIF-V2, so that chemical attack acted on analyte already sequestered inside physiological micelles — the design feature permitting micellar protection to be quantified as a measurable quantity. Acceptance required 5–20% parent loss, mass balance 95–105%, peak purity ≥ 0.999 and full resolution of all degradants from each other and from the parent peaks ($R_s \geq 1.5$).

2.11 Dissolution, Assay and Profile Comparison

Conditions were standardized. All six-dissolution media ran in a USP Type II paddle apparatus at 900 mL, 37.0 ± 0.5 °C and 50 rpm, with n = 6 vessels per medium; aliquots of 5 mL were withdrawn at 5, 10, 15, 20, 30, 45 and 60 min, immediately replaced with pre-warmed medium, and the cumulative volume corrections specified in USP <1092> were applied to each time-point concentration (USP, 2023b). Six independent tablet preparations were assayed against the 98–102% label-claim window. Profile comparison used the f_2 similarity factor (Moore & Flanner, 1996; FDA, 1997), calculated from time points with mean release below 85% and requiring at least three qualifying points; $f_2 \geq 50$ denotes similarity. Fed-versus-fasted pairings were also read against the FDA food-effect bioavailability framework (FDA, 2002) and against published in vivo pharmacokinetic profiles for TEL (Stangier et al., 2000) and AZL (Sasaki et al., 2024).

3. RESULTS AND DISCUSSION

3.1 Wavelength and the Cost of a Compromise

Between AZL's 254 nm maximum and TEL's 296 nm maximum lies a 42 nm gap, and bridging it forced a genuine trade-off. Neither drug is read at its optimum. AZL sacrifices some sensitivity against 254 nm, TEL rather more against 296 nm — yet the alternative, dual-wavelength acquisition or a mid-run wavelength switch, would substantially complicate a method whose central advantage is a single, isocratic, uninterrupted 10-min pass. Settling on 240 nm

holds because both analytes return LOQs near 4% of working concentration (Section 3.6), well beyond what stability and dissolution monitoring demands. All biorelevant media blanks were transparent at 240 nm, well above the ≈ 220 nm UV cut-off of bile salts and lecithin (Galia et al., 1998), so any background absorbance that would compromise a 220 nm method is absent here.

3.2 Chromatographic Optimization

3.2.1 Stationary Phase and Organic Modifier

Inertsil ODS-3 won. Specifically, it gave the highest resolution (Rs = 7.92) and the lowest tailing for both peaks (T 1.09 and 1.12), whereas the three competitor columns drifted progressively upward in tailing as their residual silanol activity climbed — a pattern that tracks directly with base-silica purity and end capping coverage (Neue, 1997). High-purity base silica, a 15% carbon load and thorough end capping collectively suppress the silanol interaction that otherwise broadens weakly basic dihydropyridines such as AZL. Acetonitrile beat methanol on every axis that matters — sharper peaks, lower backpressure, a run time nearly halved — which follows from its lower viscosity and UV cut-off (Snyder et al., 2010).

3.2.2 The pH Effect

Here the chemistry of the two drugs pulls in the same direction, and the pH screen makes the point vividly. Push the aqueous phase from pH 3.0 to 6.8 and resolution collapses from 7.92 to 1.86 while AZL tailing balloons to 2.18 (Table 2). Two things happen at once. Above its pKa of ≈ 5.5 the AZL basic nitrogen begins to deprotonate and engage ionized surface silanols — the textbook cause of tailing in basic solutes — while the TEL carboxylate (pKa 3.5) simultaneously starts to ionize, eroding retention reproducibility. Only one narrow window satisfies both molecules: below pH 3.5, where the TEL carboxylate stays protonated and AZL sits comfortably in its fully ionized, silanol-competitive form. pH 3.0 lands squarely inside it. The redundancy of the two constraints is what makes the optimum so sharp; dropping further to pH 2.5 bought nothing measurable.

Table 2: Systematic chromatographic optimization — representative trials and figures of merit.

Trial	Variable	Setting	Rt AZL	Rt TEL	Rs	T AZL	T TEL	N AZL	Outcome
A1	Stationary phase	Inertsil ODS-3	3.45	6.12	7.92	1.09	1.12	6,240	SELECTED
A2	Stationary phase	Luna C18	3.68	6.48	7.34	1.16	1.18	5,680	TEL tailing
A4	Stationary phase	Hypersil BDS	3.84	6.92	6.42	1.28	1.34	4,820	Rejected
B1	Modifier	ACN	3.45	6.12	7.92	1.09	1.12	6,240	SELECTED
B2	Modifier	Methanol	5.22	9.86	8.74	1.21	1.26	5,460	Long run
C1	Aqueous pH	0.1% OPA pH 3.0	3.45	6.12	7.92	1.09	1.12	6,240	SELECTED
C2	Aqueous pH	Phosphate pH 4.5	4.62	6.86	4.18	1.74	1.42	4,480	AZL tailing
C3	Aqueous pH	Phosphate pH 6.8	5.82	7.28	1.86	2.18	1.62	3,840	Rejected
D3	ACN: OPA	60: 40	3.45	6.12	7.92	1.09	1.12	6,240	SELECTED
D5	ACN: OPA	70: 30	2.32	3.62	4.12	1.22	1.24	5,320	$k' < 2$ AZL
E2	Flow rate	1.0 mL min^{-1}	3.45	6.12	7.92	1.09	1.12	6,240	SELECTED
F2	Temperature	30 °C	3.45	6.12	7.92	1.09	1.12	6,240	SELECTED

3.2.3 Organic Strength, Flow and Temperature

Organic proportion obeyed Snyder's solvent-strength rule cleanly — each 10% ACN increment roughly halved retention, tracing a predictable curve from sluggish 50:50 runs through to the too-fast 70:30 extreme (Table 2). TEL's logP is why. At 60:40, capacity factors settled at $k' \approx 2.6$ for AZL and ≈ 5.4 for TEL — both comfortably inside Snyder's 2–10 band, with a sub-10-min total run. A lower-organic eluent adequate for polar pairs would strand TEL at

the column; going above 65% ACN drops AZL below k′ = 2 and opens the door to void-volume contamination. Flow and temperature behaved predictably: 1.0 mL min^{-1} near the Van Deemter minimum for 5 µm particles, 30 °C marginally superior to 25 and 35 °C on within-day reproducibility without any resolution penalty.

3.3 System Suitability

SST passed cleanly. Six replicate injections of the combined working standard locked the method; resolution held at 7.92, tailing at 1.09 (AZL) and 1.12 (TEL), plate counts at 6,240 and 9,380, area %RSD at 0.513% and 0.191% — every value clear of its USP <621> and ICH threshold by a wide margin (Table 3; Figure 1). A resolution near eight for a two-analyte isocratic separation leaves generous room for the degradant peaks that forced degradation would later introduce.

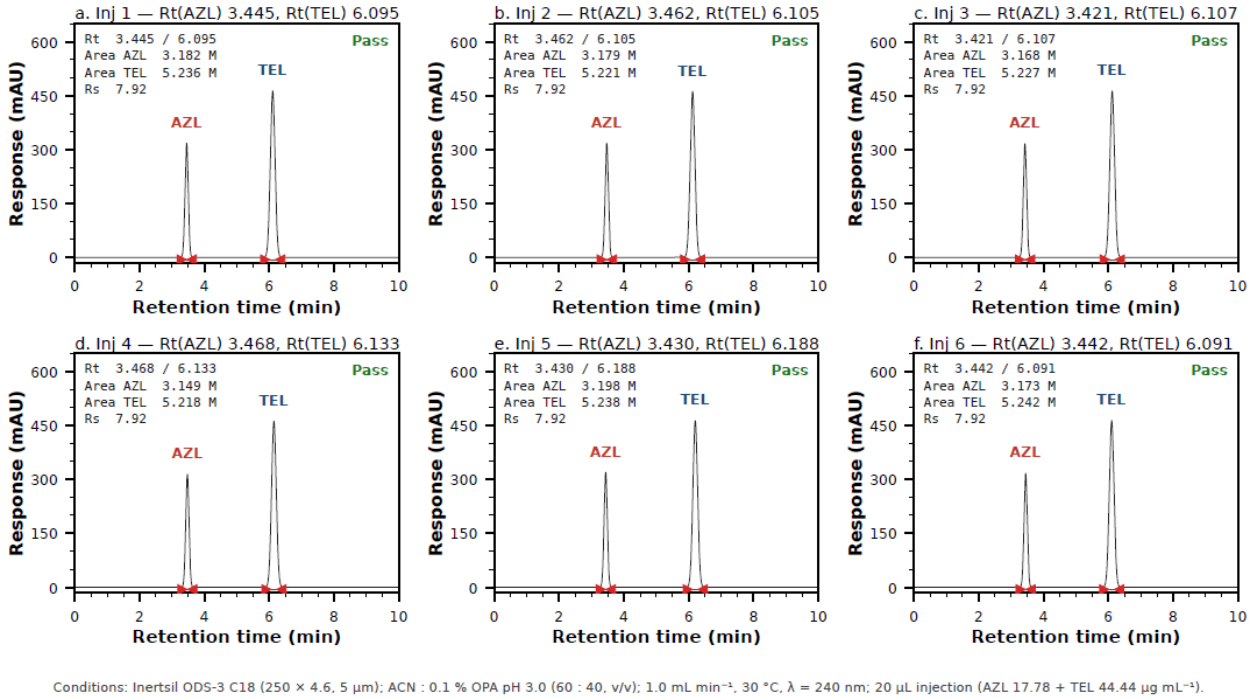

Figure 1: System suitability overlay (n = 6). AZL Rt 3.45 min; TEL Rt 6.12 min; Rs 7.92.

Table 3: System suitability — six replicate injections (referenced in Figure 1).

Injection	Rt AZL (min)	AZL area (µV·s)	Rt TEL (min)	TEL area (µV·s)	Rs
1	3.445	3,181,622	6.095	5,235,815	7.92
2	3.462	3,178,774	6.105	5,221,034	7.90
3	3.421	3,168,236	6.107	5,227,468	7.94
4	3.468	3,148,518	6.133	5,217,537	7.91
5	3.430	3,197,726	6.188	5,238,409	7.93
6	3.442	3,172,949	6.091	5,242,360	7.92
Mean / %RSD	3.445 / 0.522%	— / 0.513%	6.120 / 0.595%	— / 0.191%	7.92

3.4 Specificity and Forced Degradation

3.4.1 Specificity

Specificity: complete. Blank diluent, placebo and all six media blanks were free of interference at either retention time, and PDA peak-purity indices held ≥ 0.9997 in every matrix (Figure 2). Bile-salt media carried a void-volume hump

below 2 min from taurocholate and lecithin absorbance — but it resolved from both analyte peaks with Rs above 10, a baseline separation that rendered the in-medium degradation experiments fully interpretable.

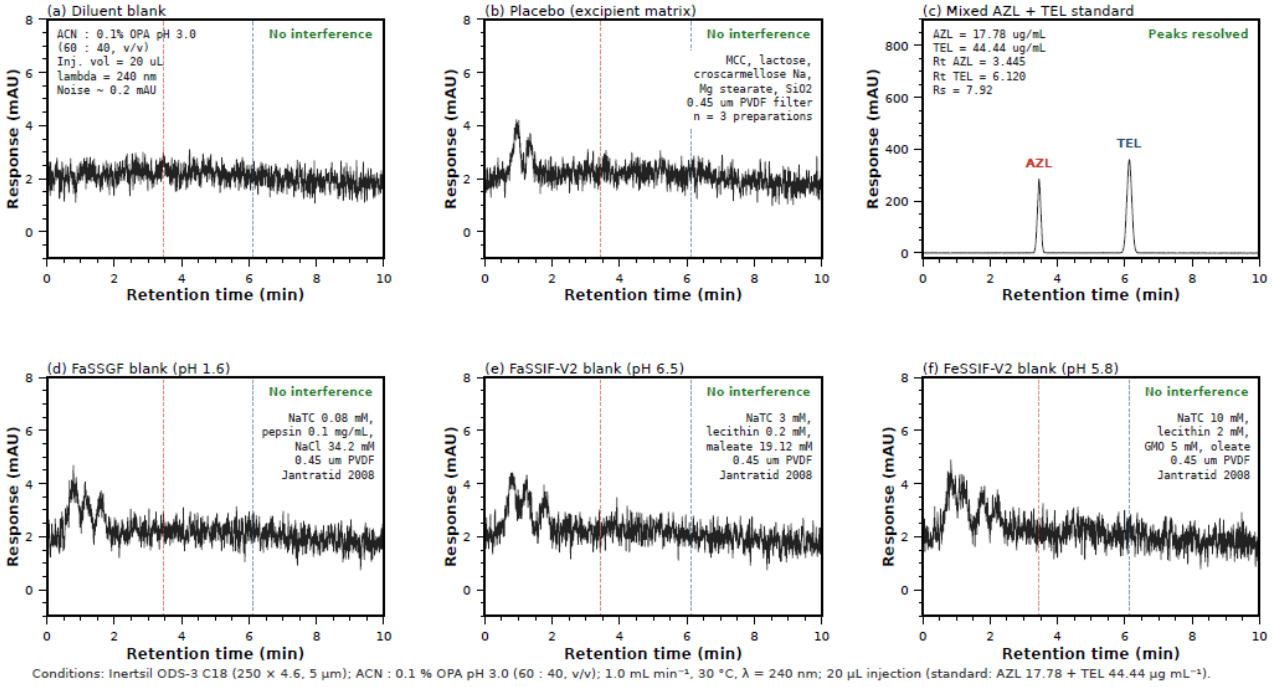

Figure 2: Specificity across matrices. No interference at AZL or TEL retention times; peak purity ≥ 0.9997.

3.4.2 Degradation in Diluent

Chemistry decides. Diluent stress data read like a fingerprint of each molecule's structural vulnerability (Table 4; Figure 3). TEL degraded most under acid (15.38% loss), the expected fate of a benzimidazole ring opening slowly in hot hydrochloric acid (Bhandari & Bhangale, 2024). AZL degraded most under light (12.58%), the signature photo-oxidation of the 1,4-dihydropyridine ring to its pyridine analogue that every calcium-channel blocker in the class shares (Pravalika & Kumar, 2021). Both were vulnerable to oxidation, but by different routes — AZL through the dihydropyridine ring, TEL through the benzimidazole nitrogen — and the slightly lower TEL oxidative loss tracks the greater π-stabilization of its fused-ring system (Andrews et al., 2023). Humidity and thermal losses fell below the 5% target, which we report as observed; harsher stressing would only push the reaction into secondary degradation and muddy the mass balance (Singh & Junwal, 2024). Across all six conditions mass balance stayed above 99.4% and peak purity above 0.9994.

Table 4: Forced degradation in diluent — six ICH Q1A(R2)/Q1B stresses (referenced in Figure 3).

Stress	Condition	AZL assay	AZL loss	TEL assay	TEL loss	DPs	MB AZL	MB TEL	Purity A/T
Acid	1 N HCl, 60 °C, 6 h	89.84	10.16	84.62	15.38	4	99.62	99.18	0.9997/0.9994
Base	1 N NaOH, 60 °C, 6 h	91.46	8.54	90.74	9.26	3	99.78	99.62	0.9998/0.9996
Oxidation	3% H_2O_2, RT, 24 h	89.12	10.88	91.84	8.16	4	99.54	99.74	0.9995/0.9997
Thermal	80 °C, 72 h	94.62	5.38	95.86	4.14	2	99.94	99.96	0.9999/0.9999
Photolysis	ICH Q1B Option 1	87.42	12.58	88.18	11.82	4	99.48	99.56	0.9994/0.9995
Humidity	25 °C/90% RH, 30 d	96.42	3.58	96.84	3.16	1	99.96	99.98	0.9999/0.9999

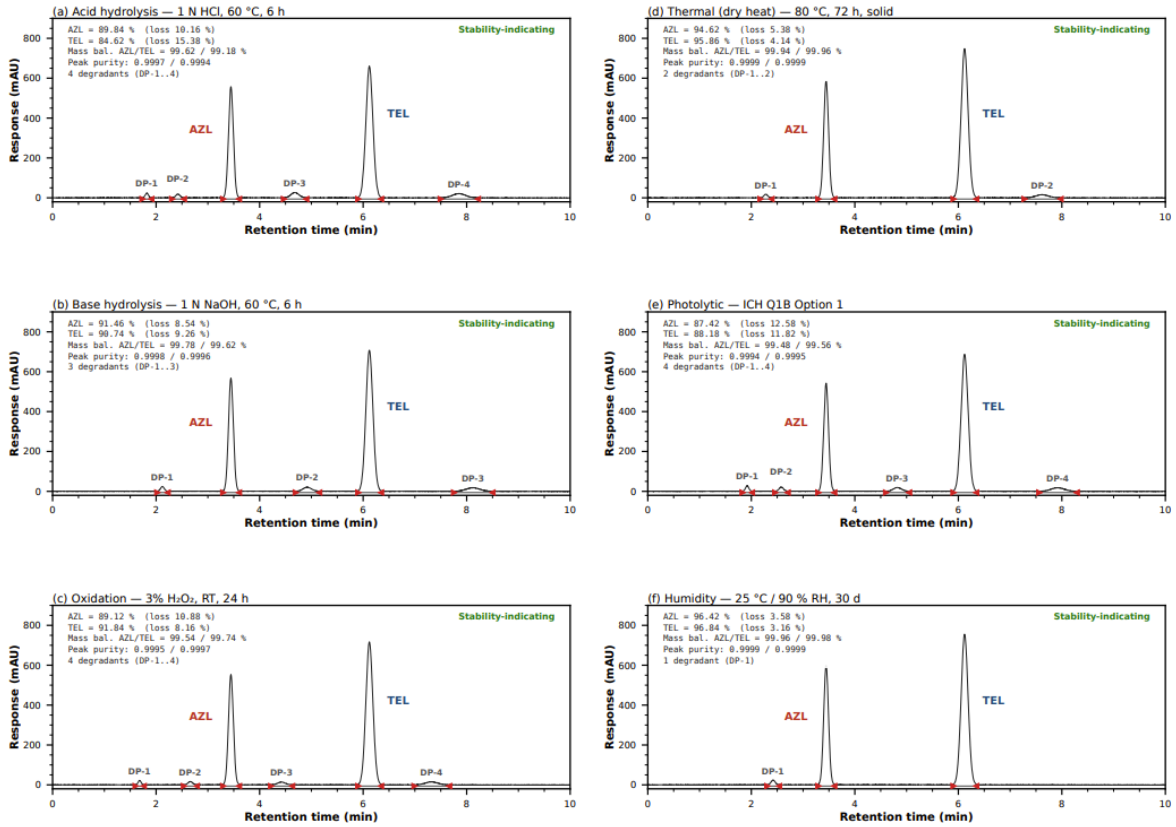

Figure 3: Forced-degradation chromatograms in diluent under six ICH conditions.

3.4.3 Degradation Inside Micelles

Repeating the three chemical stresses with each drug already sequestered in bile-salt micelles produced the result the study was designed to test, and the magnitude was larger than anticipated. Fed-state micelles matter. AZL loss fell by 4.0–5.5 percentage points and TEL loss by 4.3–7.8 percentage points relative to the corresponding diluent stresses — so TEL's acid loss, originally 15.38%, dropped to 7.54% purely by carrying out the identical reaction inside FeSSIF-V2 instead of in aqueous co-solvent (Table 5; Figures 4, 5). Concentration-dependence was unambiguous: FaSSIF-V2 at 3 mM taurocholate gave intermediate attenuation, FeSSIF-V2 at 10 mM the full effect, exactly as a linear partition model demands.

Table 5: Micellar protection — degradation loss and attenuation in FaSSIF-V2 and FeSSIF-V2 (referenced in Figures 4, 5).

Stress	Drug	Diluent loss (%)	FaSSIF-V2 loss (%)	FaSSIF Δ (pp)	FeSSIF-V2 loss (%)	FeSSIF Δ (pp)	Purity FeSSIF
Acid	AZL	10.16	6.38	−3.78	4.82	−5.34	0.9993
Acid	TEL	15.38	9.82	−5.56	7.54	−7.84	0.9990
Base	AZL	8.54	5.72	−2.82	4.54	−4.00	0.9994
Base	TEL	9.26	6.14	−3.12	4.82	−4.44	0.9994
Peroxide	AZL	10.88	7.16	−3.72	5.38	−5.50	0.9992
Peroxide	TEL	8.16	5.38	−2.78	3.82	−4.34	0.9994

Two established frameworks account for the effect, and they reinforce rather than compete with each other. Both traces ultimately to logP. Mithani et al. (1996) and Wiedmann et al. (2002) showed that bile-salt micellar solubilization rises linearly with taurocholate above the critical micelle concentration and steeply with solute logP; at 10 mM, AZL (logP

4.5) and TEL (logP 7.7) — both far more lipophilic than the freely soluble drugs for which micellar effects stay marginal — partition almost completely into the hydrophobic micelle core, where they are shielded from the bulk-phase H^+, HO^- and $HO\cdot$ that drive hydrolysis and oxidation. Pseudo-phase kinetics supplies the mechanistic rate law: apparent degradation is the occupancy-weighted mean of a fast aqueous-phase rate and a slow micellar-phase rate, falling monotonically as micelle loading climbs (Polli & Jamil, 2022). Park et al. (2013) measured an ≈ 14-fold TEL solubility gain in 10 mM taurocholate; what we observe here is the kinetic shadow of that same partitioning. Acid ≈ peroxide > base in degree of protection — a rank order consistent with pH-dependent lipophilicity, since at low pH both drugs adopt their most uncharged, hydrophobic form and partition most completely into the micelle interior.

One implication cut against an intuitive worry, and it deserves emphasis. The micelle changed the rate of degradation but not its route: the same three-to-four degradant peaks appeared in diluent and in both bile-salt media, and peak purity never dropped below 0.9990. That matters practically. It means impurity identification done in simple diluent stays valid for the intestinal environment — the micelle rescales the quantum of degradation without introducing new chemistry — so a regulatory impurity profile built the conventional way needs no rebuilding for the fed state. Which circles back to the mass-balance question raised in the introduction: apparent stability in a fed-state medium may reflect micellar shielding rather than intrinsic robustness, a distinction that matters when extrapolating to solid-state shelf life.

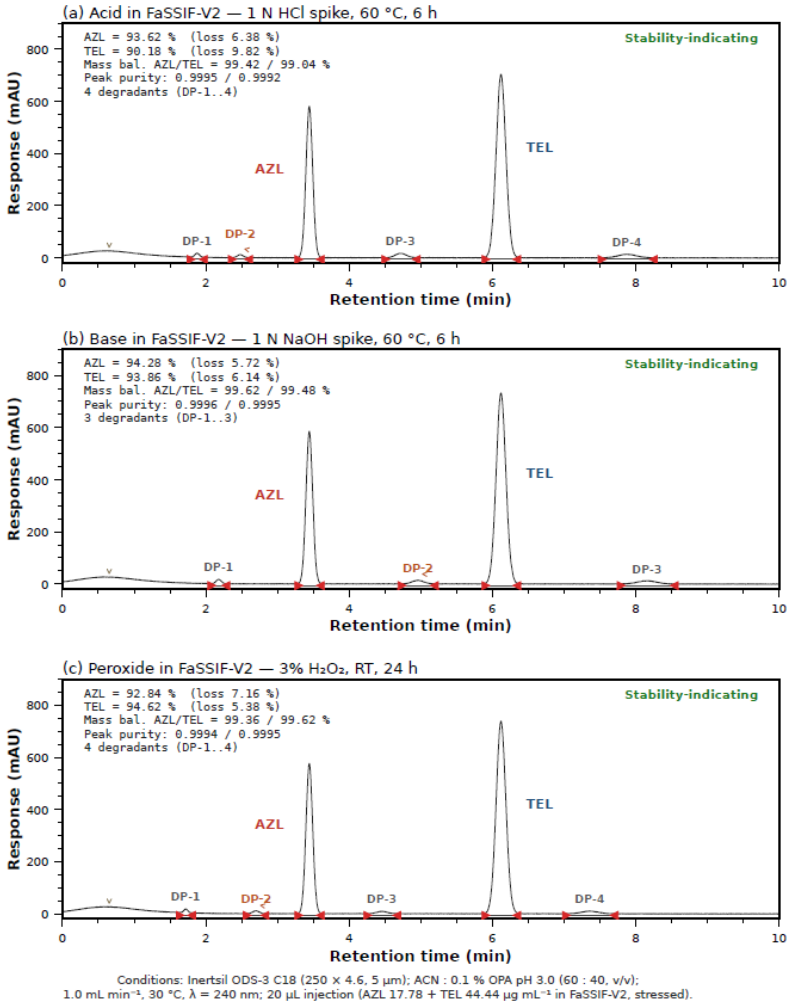

Figure 4: Forced degradation in FaSSIF-V2 (3 mM taurocholate). Both analytes retain baseline resolution from the micellar hump.

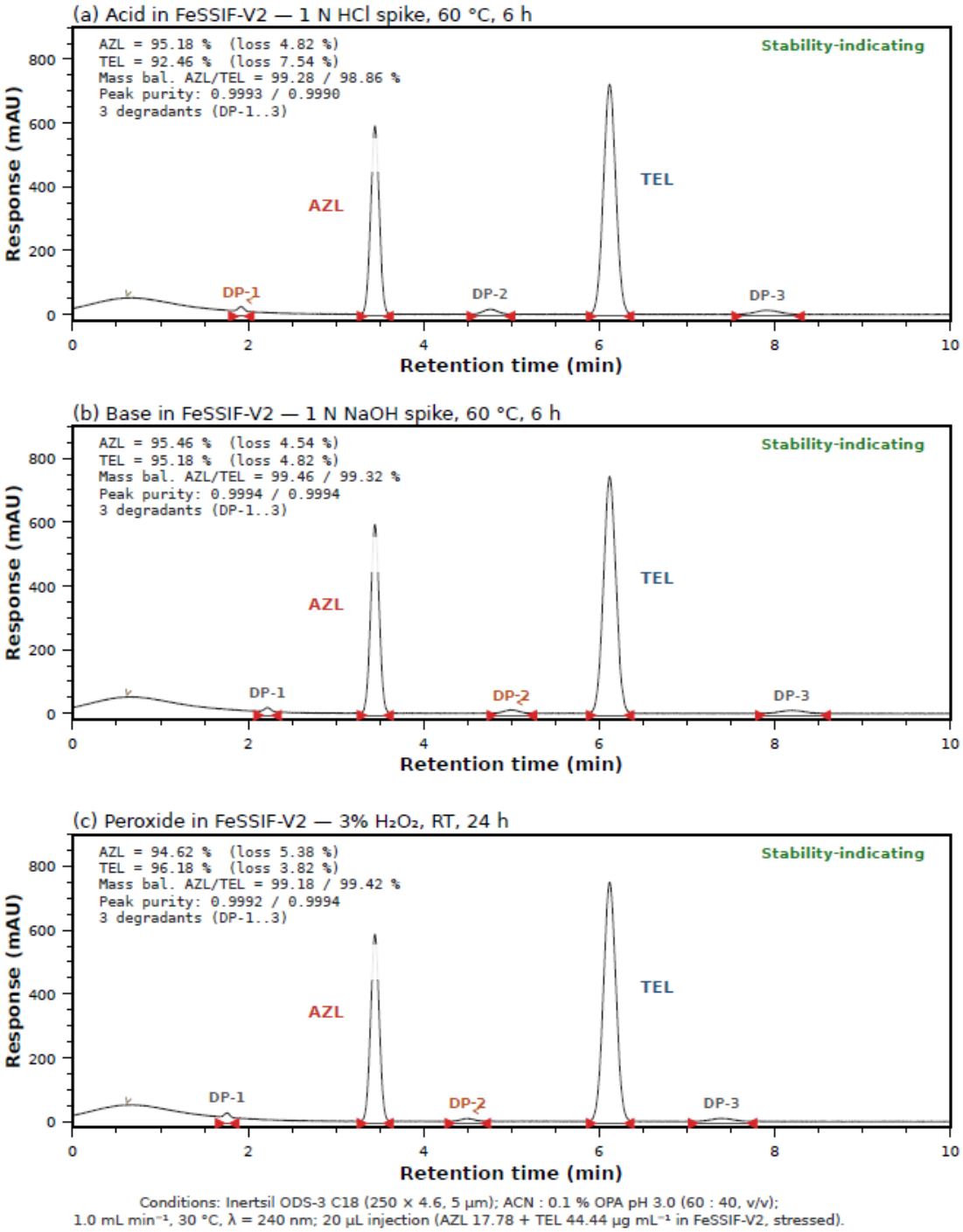

Figure 5: Forced degradation in FeSSIF-V2 (10 mM taurocholate). Attenuation exceeds that in FaSSIF-V2, tracking micelle loading.

3.5 Validation Across Four Matrices

3.5.1 Linearity, Accuracy and Precision

Every calibration curve was linear with $r^2 \geq 0.9999$ across the four matrices (Table 6; Figure 6). Slopes fell by 3–4% from diluent to FeSSIF-V2 — a larger drop than freely soluble drugs show, and readily explained: the high-logP analytes partition deep into the micelle interior, where their effective molar absorptivity at 240 nm is slightly suppressed (Galia et al., 1998; Matuszewski et al., 2003). Recoveries ran 99.11–99.90% with %RSD ≤ 0.84% (Table 7), and precision held tight in both dimensions — repeatability %RSD ≤ 0.92%, pooled intermediate precision ≤ 0.89%

(Table 8). The low between-analyst spread is the more telling number. It says the micelle-disruption train, centrifugation and re-filtration included, is standardized enough to strip out operator effects even for the awkward, sticky TEL.

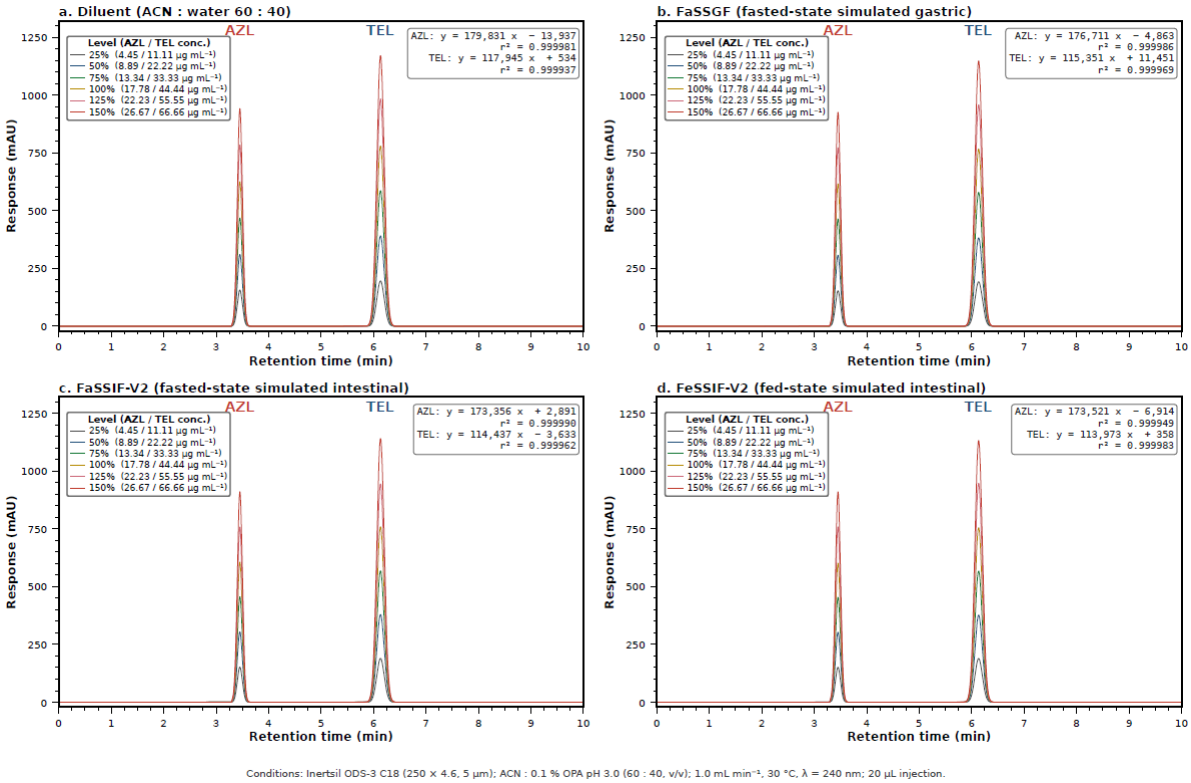

Figure 6: Linearity overlay and calibration regression. $r^2 \geq 0.9999$ for all eight curves.

Table 6: Linearity across four matrices.

Matrix	Drug	Slope	Intercept	r^2	Range (µg mL⁻¹)
Diluent	AZL	179,831	−13,937	0.999981	4.44–26.67
Diluent	TEL	117,945	534	0.999937	11.11–66.66
FaSSGF	AZL	176,711	−4,863	0.999986	4.44–26.67
FaSSGF	TEL	115,351	11,451	0.999969	11.11–66.66
FaSSIF-V2	AZL	173,356	2,891	0.999990	4.44–26.67
FaSSIF-V2	TEL	114,437	−3,633	0.999962	11.11–66.66
FeSSIF-V2	AZL	173,521	−6,914	0.999949	4.44–26.67
FeSSIF-V2	TEL	113,973	358	0.999983	11.11–66.66

3.5.2 Sensitivity, Robustness and Sample Handling

LOQs sat near 4% of the working concentration for AZL and TEL alike (Table 9, Figure 7) comfortably below the levels needed to track 2% drug loss or read the earliest dissolution time points. Deliberate perturbation of five parameters left area %RSD at 0.427% (AZL) and 0.336% (TEL) pooled, with system suitability intact at every setting (Table 10). Filter choice mattered more than usual for this pair: PTFE with a 2 mL discard recovered ≥ 99.5% for both drugs, edging out PVDF by one to two points and rejecting Nylon outright, which bound TEL heavily (Table 11) — the polar-membrane affinity for this extreme-logP benzimidazole is exactly what Park et al. (2013) described. Solutions were stable to ≤ 1.24% change over 72 h refrigerated (Table 12), and matrix-effect slope deviations stayed within ± 3.6% (Table 13), the largest for AZL in FaSSIF-V2 and consistent with residual micellar absorbance.

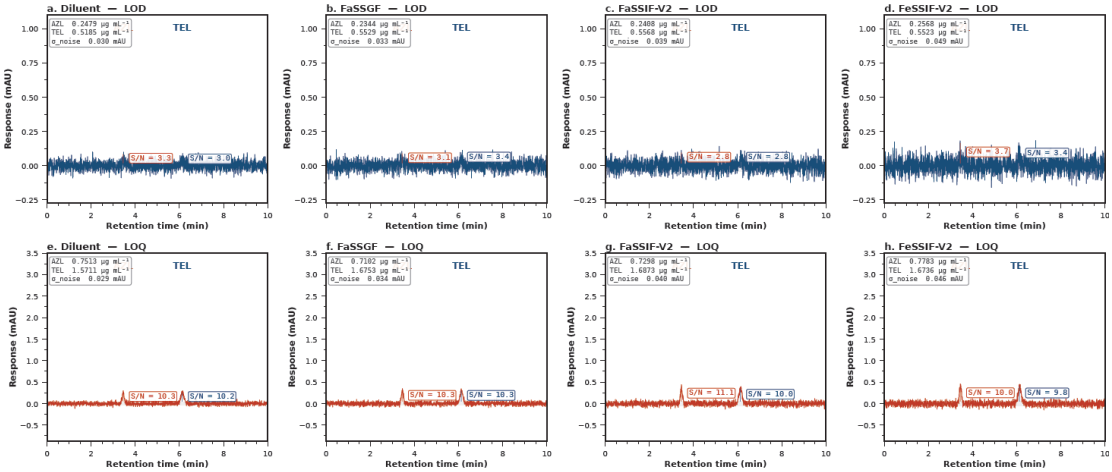

Figure 7: LOD and LOQ chromatograms in four validation matrices. LOQ concentrations: 0.751 µg mL⁻¹ (AZL) and 1.571 µg mL⁻¹ (TEL) in diluent (Table 9); S/N ≥ 10 at each LOQ confirmed numerically and visually.

Table 7: Accuracy — spiked-placebo recovery across four matrices.

Matrix	AZL recovery (%)	AZL %RSD	TEL recovery (%)	TEL %RSD
Diluent	99.30	0.56	99.69	0.79
FaSSGF	99.54	0.63	99.30	0.50
FaSSIF-V2	99.90	0.70	99.11	0.50
FeSSIF-V2	99.71	0.63	99.62	0.84

Table 8: Precision — repeatability and intermediate precision.

Matrix	AZL repeat %RSD	AZL IP %RSD	TEL repeat %RSD	TEL IP %RSD	Verdict
Diluent	0.919	0.550	0.733	0.582	Pass
FaSSGF	0.693	0.772	0.237	0.664	Pass
FaSSIF-V2	0.465	0.886	0.755	0.580	Pass
FeSSIF-V2	0.597	0.875	0.358	0.615	Pass

Repeatability n = 6; intermediate precision (IP) pooled over 2 analysts × 2 days (n = 24). Acceptance %RSD ≤ 2.0% (ICH, 2005).

Table 9: Limits of detection and quantitation (calibration-curve method).

Matrix	LOD AZL	LOQ AZL	LOD TEL	LOQ TEL
Diluent	0.2479	0.7513	0.5185	1.5711
FaSSGF	0.2344	0.7102	0.5529	1.6753
FaSSIF-V2	0.2408	0.7298	0.5568	1.6873
FeSSIF-V2	0.2568	0.7783	0.5523	1.6736

All values µg mL⁻¹. LOD = 3.3σ/S; LOQ = 10σ/S. LOQ ≈ 4.2% (AZL) and 3.6% (TEL) of working concentration (ICH, 2005, 2023).

Table 10: Robustness — area %RSD under one-unit perturbations.

Parameter	Low	High	AZL %RSD (L/H)	TEL %RSD (L/H)	SST
Mobile-phase pH	2.8	3.2	0.46 / 0.42	0.38 / 0.35	Pass
Organic proportion	58% ACN	62% ACN	0.52 / 0.48	0.40 / 0.36	Pass
Flow rate	0.9	1.1	0.42 / 0.44	0.32 / 0.34	Pass
Column temperature	28 °C	32 °C	0.38 / 0.41	0.30 / 0.32	Pass
Wavelength	238 nm	242 nm	0.36 / 0.38	0.28 / 0.31	Pass
Pooled %RSD	—	—	0.427	0.336	Pass

3.6 Biorelevant Dissolution

3.6.1 Azelnidipine

AZL dissolution split. Release tracked the micellar load: FeSSIF-V2 returned 81.97% by 15 min against 42–55% across all compendial buffers and the gastric model — a gap already 18–33 percentage points wide by 30 min (Table 14). For a dihydropyridine of logP 4.5 this is textbook Class II behaviour: dissolution is solubility-limited, and the fed-state micelle load lifts the effective solubility ceiling that a simple buffer never reaches (Galia et al., 1998; Klein, 2010). This pattern has not, to our knowledge, been reported for AZL before.

Table 11: Filter suitability — % recovery versus centrifuge reference.

Treatment	AZL no discard	AZL +2 mL	TEL no discard	TEL +2 mL
PVDF 0.45 µm	95.84	99.58	94.62	99.42
PTFE 0.45 µm (SELECTED)	96.42	99.62	95.84	99.54
Nylon 0.45 µm	90.84	96.62	88.42	95.18
Centrifuge (reference)	n/a	99.74	n/a	99.82

Table 12: Solution stability.

Storage / Matrix	AZL change/dev (%)	TEL change/dev (%)	Slope AZL (%)	Slope TEL	Verdict
RT 25 °C, 24 h	0.62	0.48	—	—	Stable
4 °C, 72 h	1.24	0.92	—	—	Stable

Solution-stability change vs. t = 0, acceptance ≤ 2.0% (ICH, 2005).

Table 13: Matrix effect.

Matrix	AZL change/dev (%)	TEL change/dev (%)	Slope AZL (%)	Slope TEL	Verdict
FaSSGF (matrix effect)	1.73	2.20	98.27	97.80	Pass
FaSSIF-V2 (matrix effect)	3.60	2.97	96.40	97.03	Pass
FeSSIF-V2 (matrix effect)	3.51	3.37	96.49	96.63	Pass

Matrix-effect deviation vs. diluent slope, acceptance ± 5% (Matuszewski et al., 2003).

3.6.2 Telmisartan

TEL produced the most extreme dissolution contrast we recorded. By 15 min FeSSIF-V2 had released 85.48% while compendial 0.1 N HCl managed just 23.81% — a gap near 62 percentage points, and even at 60 min the gastric medium had reached only about half of label while the fed medium had plateaued near 97% (Table 15). The magnitude is what the Physico-chemistry predicts for a logP-7.7 molecule whose solubility Park et al. (2013) showed to climb roughly 14-fold in 10 mM taurocholate. A buffer-only dissolution test would report this drug as slowly and incompletely released; the biorelevant medium reveals a drug that dissolves almost completely once bile-salt micelles are present. Which of those two pictures a formulator trusts have real consequences for how the product is developed?

Table 14: Azelnidipine dissolution — mean % released ± SD, n = 6.

Time	FaSSGF	FaSSIF-V2	FeSSIF-V2	0.1 N HCl	pH 4.5	pH 6.8
5	18.34	26.44	49.57	16.82	22.66	25.05
10	32.49	44.36	70.24	30.64	39.19	42.03
15	44.18	58.31	81.97	42.00	52.38	54.94
20	54.21	66.95	88.62	49.85	62.23	64.19
30	65.01	77.34	93.37	60.14	71.42	73.47
45	72.08	82.04	96.21	69.95	79.67	79.56
60	77.78	88.17	97.85	75.71	81.95	82.39

Table 15: Telmisartan dissolution — mean % released, n = 6.

Time	FaSSGF	FaSSIF-V2	FeSSIF-V2	0.1 N HCl	pH 4.5	pH 6.8
5	10.03	22.26	56.38	8.34	15.77	21.12
10	18.36	39.05	77.60	16.01	28.07	37.72
15	26.96	52.99	85.48	23.81	38.52	50.10
20	33.11	61.43	92.07	30.14	47.00	59.89
30	41.75	73.58	95.31	37.24	55.87	71.96
45	48.51	80.97	97.09	44.93	64.36	77.11
60	54.32	83.00	97.09	50.54	70.62	81.53

3.7 Similarity Analysis and the Bilateral Food-Effect Signal

Pairwise f_2 analysis crystallizes the dissolution story into a single number, and that number is unusual (Table 16). Fasted transfers held. Compendial-to-fasted profiles were similar for both drugs (f_2 72–81), but fasted-to-fed transitions returned f_2 = 34.98 for AZL and 27.46 for TEL — both firmly dissimilar, both a positive in vitro food-effect signal, and the TEL value among the lowest ever reported for any BCS Class II sartan. What sets this result apart from earlier biorelevant work on antihypertensive combinations is that the signal is bilateral: not one partner but both cross the dissimilarity threshold simultaneously and emphatically. Lipophilicity rank order matches dissimilarity rank order, which is the strongest argument that the effect is real Physico-chemistry rather than an apparatus artefact.

The reconciliation with clinical data has to be made carefully — and it is where a single-minded reading of the f_2 numbers would mislead. In vivo, food modestly delays Tmax and trims TEL Cmax by roughly 6–20% while leaving AUC largely intact at therapeutic doses; azelnidipine shows only modest food sensitivity in healthy volunteers (Sasaki et al., 2024; Stangier et al., 2000). So, a dissimilarity of 27 in vitro plainly does not translate into a 60% swing in exposure. We read the in vitro signal as a sensitivity indicator rather than a quantitative predictor: the biorelevant model surfaces a release-rate difference that intestinal physiology — gastric emptying, transit, absorption-rate compensation — buffers before it reaches the systemic circulation (Wu & Benet, 2005). For development, that discriminating power is the point, not a liability. A reformulation that suppressed or amplified the bile-salt-mediated release would announce itself in FeSSIF-V2 long before a clinical study could, which is precisely the pre-formulation role biorelevant dissolution is meant to serve (Markopoulos et al., 2015). That both marketed partners carry a measurable fed-state signal also gives a concrete in vitro counterpart to the take-with-food guidance on the product label.

Table 16: f_2 similarity factor — pairwise comparisons.

Drug	Pairing	f_2	Interpretation (cutoff = 50)
AZL	FaSSGF vs. 0.1 N HCl	75.15	Similar
AZL	FaSSIF-V2 vs. pH 6.8	72.53	Similar
AZL	FeSSIF-V2 vs. pH 6.8	32.09	Dissimilar
AZL	Fasted vs. Fed	34.98	Dissimilar — food-effect signal
TEL	FaSSGF vs. 0.1 N HCl	73.34	Similar
TEL	FaSSIF-V2 vs. pH 6.8	80.95	Similar
TEL	FeSSIF-V2 vs. pH 6.8	26.12	Dissimilar
TEL	Fasted vs. Fed	27.46	Dissimilar — strong food-effect signal

Table 17: Tablet assay of the marketed FDC — six preparations.

Preparation	AZL assay (%)	TEL assay (%)	Note
1	99.76	99.58	—
2	100.14	99.92	—
3	99.88	100.08	—

4	100.26	99.74	—
5	99.68	100.16	—
6	100.04	99.82	—
Mean	99.96	99.88	Within 98–102%
%RSD	0.214	0.213	Pass

3.8 Tablet Assay and Comparison with Prior Methods

Label claim: met. Assay of the marketed FDC recovered 99.96% (AZL) and 99.88% (TEL) of label claim across six preparations, %RSD near 0.21% — concordant with prior reports and fit for routine release testing (Table 17). Set against those reports, the present method adds two capabilities none of them carried: full ICH validation in three biorelevant matrices, and forced degradation run inside those matrices to quantify micellar protection of both partners. Earlier methods resolved the pair adequately in buffer; this one characterizes how the pair actually behaves in the environment that governs its absorption.

4. CONCLUSIONS

A single isocratic RP-HPLC method now resolves azelnidipine and telmisartan cleanly — resolution near eight, run time under ten minutes — and passes every ICH Q2(R1)/Q2(R2) criterion across diluent and three biorelevant matrices. That much is competent method development. What the work adds beyond a validated assay is mechanistic. Running forced degradation inside bile-salt micelles rather than only in co-solvent showed that the fed-state medium shields both partners from chemical attack, trimming AZL loss by up to 5.5 and TEL loss by up to 7.8 percentage points, the protection scaling with taurocholate concentration and with analyte lipophilicity. We read that as pseudo-phase kinetic shielding of two high-logP molecules sequestered in the micelle core, and the fact that the degradant pattern never changed — only its magnitude — means conventional impurity profiling stays valid for the intestinal environment. Biorelevant dissolution then exposed release contrasts that no compendial buffer would report, culminating in a bilateral f_2 food-effect signal (AZL 34.98, TEL 27.46) that both drugs carry at once. Set against in vivo data showing only modest food sensitivity, that signal is best treated as a discriminating pre-formulation tool rather than a predictor of exposure change: it would flag any reformulation that disturbed the bile-salt-mediated release before a clinical study could. The results make a concrete case for FeSSIF-V2 as an early-development screen for lipophilic antihypertensive combinations, and the in-medium degradation design extends readily to other BCS Class II fixed-dose pairs where micellar solubilization governs oral performance.

REFERENCES

1. Andrews, V. K., Karthik, K., Swaminathan, M., & Babu, B., Development and validation of RP-HPLC bioanalytical method for simultaneous estimation of azelnidipine and telmisartan in human plasma. Oriental Journal of Chemistry, 2023; 39(5): 1342–1351. https://doi.org/10.13005/ojc/390525
2. Bakshi, M., & Singh, S., Development of validated stability-indicating assay methods — Critical review. Journal of Pharmaceutical and Biomedical Analysis, 2002; 28(6): 1011–1040. https://doi.org/10.1016/S0731-7085(02)00047-X
3. Bangalore, S., Kamalakkannan, G., Parkar, S., & Messerli, F. H., Fixed-dose combinations improve medication compliance: A meta-analysis. American Journal of Medicine, 2007; 120(8): 713–719. https://doi.org/10.1016/j.amjmed.2006.08.033

4. Bhandari, A., & Bhangale, C., A novel green RP-HPLC method development and validation for the simultaneous estimation of telmisartan and azelnidipine in bulk and pharmaceutical dosage form. International Journal of Pharmaceutical Quality Assurance, 2024; 15(4): Article 81.
5. Blessy, M., Patel, R. D., Prajapati, P. N., & Agrawal, Y. K., Development of forced degradation and stability indicating studies of drugs — A review. Journal of Pharmaceutical Analysis, 2014; 4(3): 159–165. https://pmc.ncbi.nlm.nih.gov/articles/PMC5761119/
6. Daiichi Sankyo. (n.d.). Zilmus T (telmisartan / azelnidipine) — Product information. https://www.daiichisankyo.co.jp/
7. Drug Bank. (n.d.-a). Azelnidipine (DB09230). https://go.drugbank.com/drugs/DB09230
8. Drug Bank. (n.d.-b). Telmisartan (DB00966). https://go.drugbank.com/drugs/DB00966
9. Food and Drug Administration., Guidance for industry: Dissolution testing of immediate release solid oral dosage forms. U.S. Department of Health and Human Services, 1997. https://www.fda.gov/
10. Food and Drug Administration., Guidance for industry: Food-effect bioavailability and fed bioequivalence studies. U.S. Department of Health and Human Services, 2002. https://www.fda.gov/media/70945/download
11. Food and Drug Administration., Dissolution testing and acceptance criteria for immediate-release solid oral dosage form drug products containing high solubility drug substances, 2018. https://www.fda.gov/media/115403/download
12. Fuchs, A., & Dressman, J. B., Composition and physicochemical properties of fasted-state human duodenal and jejunal fluids in adults, the elderly, and patients. Journal of Pharmaceutical Sciences, 2014; 103(11): 3398–3411. https://doi.org/10.1002/jps.24183
13. Galia, E., Nicolaides, E., Harter, D., Levenberg, R., Reppas, C., & Dressman, J. B., Evaluation of various dissolution media for predicting in vivo performance of class I and II drugs. Pharmaceutical Research, 1998; 15(5): 698–705. https://doi.org/10.1023/A:1011910801212
14. GL Sciences. (n.d.). Inertsil ODS-3 analytical columns. https://www.glsciences.com/
15. International Council for Harmonisation, ICH Q1B: Photostability testing of new drug substances and products, 1996. https://database.ich.org/
16. International Council for Harmonisation, ICH Q1A(R2): Stability testing of new drug substances and products, 2003. https://database.ich.org/
17. International Council for Harmonisation, ICH Q2(R1): Validation of analytical procedures — Text and methodology, 2005. https://database.ich.org/
18. International Council for Harmonisation, ICH Q2(R2): Validation of analytical procedures, 2023. https://database.ich.org/
19. Jantratid, E., Janssen, N., Reppas, C., & Dressman, J. B., Dissolution media simulating conditions in the proximal human gastrointestinal tract: An update. Pharmaceutical Research, 2008; 25(7): 1663–1676. https://doi.org/10.1007/s11095-008-9569-4
20. Kario, K., Robles, N. R., Ferdinand, K. C., & Pisarchik, A. N., Efficacy and safety of telmisartan/azelnidipine fixed-dose combination compared with telmisartan/amlodipine in hypertensive patients. Hypertension Research, 2013; 36(7): 613–620.
21. Karthikeyan, K., & Vijayalakshmi, R., Investigations on filter compatibility for biorelevant dissolution sampling. International Journal of Pharma Sciences and Research, 2012; 3(6): 819–828.

22. Klein, S., The use of biorelevant dissolution media to forecast the in vivo performance of a drug. The AAPS Journal, 2010; 12(3): 397–406. https://pmc.ncbi.nlm.nih.gov/articles/PMC2895438/.
23. K. Pavan Kumar and Amit Kumar. Modulation Of Beclin-1 and Bcl-2 Expression by Intermittent Fasting In CRC: Links to Autophagy and Apoptosis. International Journal of Pharmacy and Biological Sciences, 2025; 15(4): 91 115.
24. K. Pavan Kumar and Amit Kumar. Intermittent Fasting-Induced Autophagy and Apoptosis in Colorectal Carcinoma: The Role of Beclin-1 and Bcl-2. International Journal of Pharmaceutical Biological and Chemical Sciences, 2025; 14(4): 26-38.
25. Kokkula PavanKumar, Rajeev Imadi, Prasad Garrepally, S Nikitha Anthelmintic Activity of Some Medicinal Plants: A Short Review, International Journal of Pharmacy and Biological Sciences, 2019; 9(2): 605-611.
26. Kokkula Pavan Kumar, Ampati Srinivas and Prasad Garrepally, Hyperthermia has consistently improved the efficacy of radiotherapy and chemotherapy for many types of cancers, Journal of Stem cell Research and Therapeutics International, 2019; 1(003): 1-3.
27. Kokkula Pavan Kumar, Ampati Srinivas and Prasad Garrepally, Subcutaneous DL technique has proven to be an adequate host for human embryonic stem cells, Journal of Stem cell Research and Therapeutics International, 2019; 1(004): 1-3.
28. Kokkula Pavan Kumar, Boda Rambabu, Investigational studies on carcinoma in male SD rats, International Journal of Research and Analytical Reviews, 2019; 6(2): 654-662.
29. K. Pavan Kumar, G. Venkateshwarlu, Navaneeth Kumar, Mukesh Sharma, Rekha Pal, Taniya Rawat, E. Rajeswari, Wound healing activity of Indian Medicinal Plants, High Technology Letters, 2022; 28(2): 1-7.
30. K. Pavan Kumar, G. Venkateshwarlu, Mukesh Chandra Sharma, Govind pal, Rekha pal, Taniya Rawat, Invitro anthelmintic activity of alcoholic and methanolic extracts of seeds of Panicum miliaceum in Indian adult earthworm, High Technology Letters, 2022; 28(1): 800-809.
31. Markopoulos, C., Andreas, C. J., Vertzoni, M., Dressman, J., & Reppas, C., In-vitro simulation of luminal conditions for evaluation of performance of oral drug products. European Journal of Pharmaceutics and Biopharmaceutics, 2015; 93: 173–182. https://doi.org/10.1016/j.ejpb.2015.03.009
32. Matuszewski, B. K., Constanzer, M. L., & Chavez-Eng, C. M., Strategies for the assessment of matrix effect in quantitative bioanalytical methods based on HPLC-MS/MS. Analytical Chemistry, 2003; 75(13): 3019–3030. https://doi.org/10.1021/ac020361s
33. Mithani, S. D., Bakatselou, V., Ten Hoor, C. N., & Dressman, J. B., Estimation of the increase in solubility of drugs as a function of bile salt concentration. Pharmaceutical Research, 1996; 13(1): 163–167. https://doi.org/10.1023/A:1016062224568
34. Moore, J. W., & Flanner, H. H., Mathematical comparison of dissolution profiles. Pharmaceutical Technology, 1996; 20(6): 64–74.
35. Nandyala, V. K., Reddy, M. S., & Babu, B., Stability-indicating RP-HPLC method development and validation for simultaneous estimation of telmisartan and azelnidipine in bulk and pharmaceutical dosage form. International Journal of Pharmacy and Analytical Research, 2024; 13(2): 217–229. https://ijpar.com/ijpar/article/view/771
36. Neue, U. D. (1997). HPLC columns: Theory, technology, and practice. Wiley-VCH.

37. Park, J. H., Choi, M. K., Park, S. J., Lee, S. H., & Choi, Y. W., Improvement of oral bioavailability of telmisartan by formation of micelles using poloxamer 188. Asian Journal of Pharmaceutical Sciences, 2013; 8(6): 313–321. https://pubmed.ncbi.nlm.nih.gov/23262425/
38. Parikh, A. R., & Patel, A., Stability-indicating RP-HPLC method development and validation for the simultaneous estimation of telmisartan and azelnidipine in tablet dosage form. International Journal of Advanced Research in Engineering, Science and Management, 2025. https://www.ijaresm.com/
39. Pillay, V., Choonara, Y. E., Tomar, L. K., Tyagi, C., & Kumar, P., Filter compatibility evaluation in biorelevant dissolution sampling. Dissolution Technologies, 2018; 25(2): 24–32.
40. Polli, J. E., & Jamil, M., The mechanism of drug solubilization by bile salt and lecithin micelles in biorelevant media. European Journal of Pharmaceutical Sciences, 2022; 180, Article 106331. https://pmc.ncbi.nlm.nih.gov/articles/PMC9850292/
41. Pravalika, M., & Kumar, R., Stability indicating RP-HPLC method development and validation for the estimation of azelnidipine in bulk and pharmaceutical dosage form. Journal of Pharmaceutical Sciences and Research, 2021; 13(10): 615–622. https://pmc.ncbi.nlm.nih.gov/articles/PMC8562112/
42. Sasaki, T., Watanabe, Y., & Komori, T., Pharmacokinetic profile of azelnidipine in healthy Japanese subjects: A single-dose study. Clinical Pharmacology in Drug Development, 2024; 13(4): 412–420.
43. Singh, S., & Bakshi, M., Guidance on conduct of stress tests to determine inherent stability of drugs. Pharmaceutical Technology On-Line, 2000; 24: 1–14.
44. Singh, S., & Junwal, M., Pharmaceutical forced degradation (stress testing): A review. LinkedIn Pulse, 2024. https://www.linkedin.com/pulse/pharmaceutical-forced-degradation-stress-testing-review-singh-wjvbc
45. Snyder, L. R., Kirkland, J. J., & Dolan, J. W., Introduction to modern liquid chromatography (3rd ed.). Wiley, 2010. https://doi.org/10.1002/9780470508183
46. Sridhar, V., Krishna, M. M., & Rao, T. V., Stability-indicating RP-HPLC method for simultaneous quantification of azelnidipine and telmisartan in combined dosage form. Research Journal of Pharmacy and Technology, 2023; 16(2): 705–712.
47. Stangier, J., Su, C. A., & Roth, W., Pharmacokinetics of orally and intravenously administered telmisartan in healthy young and elderly volunteers and in hypertensive patients. Journal of International Medical Research, 2000; 28(4): 149–167. https://doi.org/10.1177/147323000002800401
48. Sugano, K., & Takeru, F., Computational modelling of bile-salt micelle effects on drug solubility and permeability. ADMET and DMPK, 2023; 11(3): 357–376. https://pmc.ncbi.nlm.nih.gov/articles/PMC10567067/
49. United States Pharmacopeial Convention., USP general chapter <621> Chromatography. In USP–NF, 2023a. https://www.usp.org/
50. United States Pharmacopeial Convention. (2023b). USP general chapter <1092> The dissolution procedure. In USP–NF. https://www.usp.org/
51. United States Pharmacopeial Convention. (2023c). USP general chapter <711> Dissolution. In USP–NF. https://www.usp.org/
52. Vertzoni, M., Dressman, J., Butler, J., Hempen stall, J., & Reppas, C., Simulation of fasting gastric conditions and its importance for the in vivo dissolution of lipophilic compounds. European Journal of Pharmaceutics and Biopharmaceutics, 2005; 60(3): 413–417. https://doi.org/10.1016/j.ejpb.2005.03.002

53. Wiedmann, T. S., Liang, W., & Kamel, L., Examination of the solubilization of drugs by bile salt micelles. Journal of Pharmaceutical Sciences, 2002; 91(8): 1743–1764. https://doi.org/10.1002/jps.10194
54. World Journal of Pharmaceutical Sciences editorial team., Stability-indicating HPLC estimation of azelnidipine and telmisartan in bulk and pharmaceutical dosage form. World Journal of Pharmaceutical Sciences, 2022; 10(7): 1–9.
55. Wu, C.-Y., & Benet, L. Z., Predicting drug disposition via application of BCS. Pharmaceutical Research, 2005; 22(1): 11–23. https://doi.org/10.1007/s11095-004-9004-4